Double co-host emitter based top emitting white organic light emitting diodes with enhanced brightness and efficiency

Neha Jain[1,2]*, Sujata Pandey[3], Rajiv Kr. Singh[4], and O. P. Sinha[5]

1. Department of ECE, Amity School of Engineering and Technology, Amity University, UP, Noida, India

2. Department of EEE, Galgotia College of Engineering and Technology, Greater Noida, India

3. Department of ECE, Amity School of Engineering and Technology, Amity University, UP, Noida, India

4. CSIR- National Physical Laboratory, New Delhi, India

5. Amity Institute of Nanotechnology, Amity University UP, Noida, India

(Received 18 November 2020; Revised 11 February 2021)

Novel and simplified bi-layer top-emitting white organic light emitting diodes (OLEDs) with dual co-host emitters have been simulated and analyzed. They consist of yellow-green emitting layer (EML) as electron transport layer (ETL) and blue EML as hole transport layer (HTL). Novelty of the device lies in simplification of tri-layer white OLED to a bi-layered device which is done by merging yellow-green EML with ETL and blue EML with HTL. The simulated devices show Commission Internationale de L'Eclairage (CIE) colour coordinates well within the emission range of white light. The results show that device A with 5,6,11,12-tetraphenylnaphthacene (rubrene) doped ETL has achieved the lowest luminance but longest excited state lifetime. Device D with tris-(8-hydroxyquinoline) aluminum: 4-(dicyanomethylene)-2-t-butyle-6-(1,1,7,7- tetra-methyljulolidyl-9-enyl)4H-pyran (Alq_3: DCJTB) as ETL which emits yellow light and 2, 7-bis [N, N-bis (4-methoxy-phenyl) amino]-9, 9-spirobifluorene (MS-TPD): bis(2-methyl-8-quninolinato)-4-phenylphenolate alu-minium (BAlq) as HTL which is responsible for blue light emission is found to have best characteristics when compared to other simulated devices. It has a maximum luminance of 10 000 cd/m^2 and current efficiency of 15.25 cd/A, respectively, and CIE coordinates are at (0.329, 0.319). The device is found to be compatible to be used in solid state lighting applications because of the low driving voltage of the device.

Document code: A **Article ID:** 1673-1905(2021)10-0581-5

DOI https://doi.org/10.1007/s11801-021-0183-6

White organic light emitting diodes (OLEDs) is getting popular because of its tremendous performance in many applications, like full colour flat panel displays, solid state lighting, back light of liquid crystal displays, sub-pixels of organic light emitting diode display etc[1,2]. White OLEDs are getting attention because of its outstanding performance that includes high power conversion efficiency, light in weight, its mechanical flexibility, high power efficacy and many more[1]. To increase the power efficacy of white OLEDs, efficient phosphorescent dyes are generally mixed together to get the desired emission colour[1,2]. The white emission from the OLEDs can be realized by different methods which includes the modelling of different structures. This includes (i) mixing of different colour dyes in a single emitting layer, (ii) using multiple emitting layers (EMLs) in a single device, (iii) single or multiple EML which composes of host and guest emitters, (iv) using a single colour emitting OLED along with down conversion layer (v) excimer/exciplex emission. Excimers are the combination of molecules or atoms that can be only formed and can exist in excited states. Exciplexes can act as both emitter and host for phosphorescent and fluorescent emitters. Out of these, mixing of different colour dyes can be categorized into two parts. They are tri-layer emitting layers and dual EMLs. Tri-layer emitting layers consist of primary red, green, and blue colour dyes, whereas dual emitting layers consists of mixing of complementary colours, such as blue and orange, yellow-green and blue etc[1-5]. Out of these two, tri-layer EML have the advantage that they have high luminance and colour rendering index (CRI). But it complicates the device structure because of the large number of emitting layers and hence obscures the fabrication process. In addition, guest emitters if used in the structure affect the CIE coordinates. When we compare the two methods (dual and tri-layer emitter structures) in terms of CIE coordinates, dual EML structure is found stable with CIE coordinates and also easy fabrication process as compared to the tri-layer EML structure. Because of the different aging rates of the emitters used

* E-mail: aceneha@gmail.com

in the mentioned methods above, it is difficult to achieve the colour stability in white OLEDs[3-7].

Emission of white colour from white OLED is dependent on thickness of the emitting layers and for fabricating an OLED, it is a difficult task to perfectly control the thickness via evaporation. It is technologically challenging to achieve white emission from such a fabricated OLED[4]. For industrial applications, luminous efficacy is more important than external quantum efficiency (EQE) as it considers power consumption and thus operating voltage. Also, for solid state lighting applications, luminous efficacy must be high at low driving voltage of the white OLED. Additionally, the efficiency of the OLEDs decreases with increasing the brightness which is called as efficiency roll-off[8,9].

In this study, we have designed and simulated structures in order to simplify the fabrication process of the device. We proposed a simple method of double carrier transport emitting layers. It consists of electron transport layer (ETL) and hole transport layer (HTL) without using extra hole injection layer (HIL) or electron injection layer (EIL). This structure consists of blue EML which also functions as HTL, and orange or yellow-green EML that functions as ETL.

In this study, we have simulated four structures. The detailed description of these structures can be explained with the help of Fig.1.

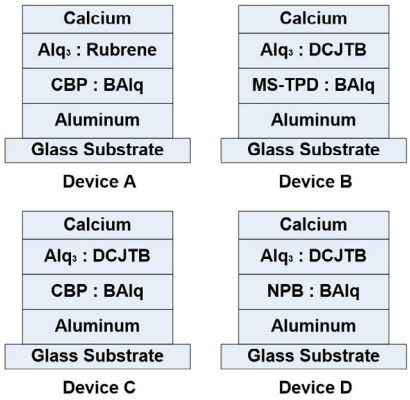

Fig.1 Top emitting white OLED structures

The white OLED structure simulated here proposed a simplified white OLED consisting of only two organic layers i.e., hole-transporting type orange or yellow-green emitting layer and electron-transporting type blue emitting layer. Here, Fig.1 shows the structures of a top-emitting white OLED, where in Device A, tris-(8-hydroxyquinoline) aluminum (Alq_3) doped with 4-(dicyanomethylene)-2-t-butyle-6-(1,1,7,7-tetramethyljulolidyl-9-enyl)4H-pyran (DCJTB) is acting as an ETL and also an orange light EML, N,N9-di(naphthalene-1-yl)-N,N9-diphenyl-benzidine (NPB) doped with bis(2-methyl-8-quninolinato)-4-henylphenolate aluminium (BAlq) is an HTL and also a blue light EML. Similarly, in Devices B, C and D, ETL is also acting as orange or yellow-green emitter (which can also be called as ET-YEML) while HTL is also acting as blue emitter (which can also be called as HT-BEML). Aluminium (Al) and calcium (Ca) are anode and cathode, respectively. Fig.1 shows the schematic device structure of Ca (20 nm)/ ET-YEML/ HT-BEML/ Al (60 nm)/ glass substrate.

Fig.2 shows the energy band diagram for different structures simulated in this paper. The white OLED with Alq_3: DCJTB (50 nm) as ET-YEML and NPB: BAlq (45 nm) as HT-BEML is referred as Device A. Device B has Alq_3: DCJTB (50 nm) as ET-YEML while CBP (50 nm) as HT-BEML. Device C consists of [Alq_3: rubrene] (100 nm) as ET-YEML while [CBP: BAlq] (50 nm) as HT-BEML whereas white OLED with [Alq_3: DCJTB] (50 nm) as ET-YEML and [MS-TPD: BAlq] (60 nm) as HT-BEML is referred as Device D.

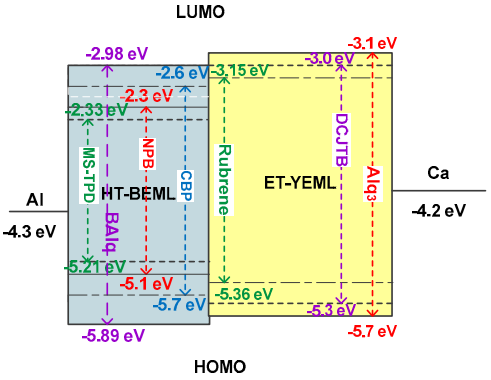

Fig.2 HOMO-LUMO structure of white OLED with HT-YEML and ET-BEML

Fig.3 shows the electroluminescence (EL) intensity curve with respect to wavelength. Intensity of light that can be emitted from a top-emitting OLED is given by[17]

$$I(\lambda,\theta)=\frac{T_t\left[1+R_b+2\sqrt{R_b}\cos\left(-\phi_b+\frac{4\pi n_{org}z_0\cos(\theta_{org,EML})}{\lambda}\right)\right]}{\left(1-\sqrt{R_bR_t}\right)^2+4\sqrt{R_bR_t}\sin^2(\Delta\phi/2)}, \quad (1)$$

where T_t is the transmittance through the top contact, R_b and R_t are the bottom and top contact reflectivity, I_0 is the intensity of the radiating molecules, and z_0 is the distance to the reflecting layer.

The EL spectrum of device A shown in Fig.3 has a yellow-green emission of Alq_3 which has an emission peak at about 485 nm and exhibits a blue emission of 4,4'-Bis(N-carbaz-olyl)-1,1'-biphenyl (CBP) when it is doped with BAlq and has an emission peak at about 610 nm. This combination of yellow-green and blue gives a white emission with CIE coordinates of (0.32, 0.336). The best white OLED characteristics of device D is due to the appropriate matching in the emission and absorption band of NPB and BAlq as can be referred from the PL and EL spectra's in Ref.[20] when compared with others. Also, CBP does not exhibit sufficient triplet level energy for energy transfer from triplet-to-

triplet states which will contribute to the degraded output of device A. Additionally, rubrene doping is found responsible for impeding the device A's performance which is further accountable for the worst EL in the same. Effect of doping with rubrene has also been investigated in further sections using *I-V* and *Z-V* characteristics[19,20].

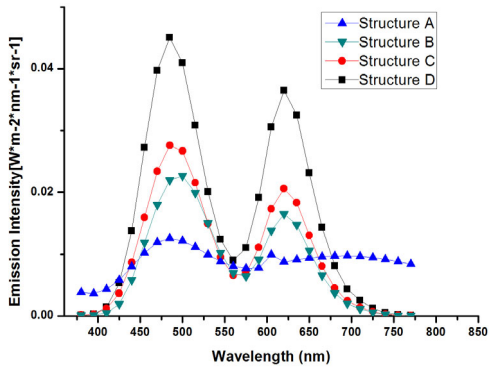

Fig.3 Electroluminesce intensity of devices

After one cycle in the structure, the light wave has a phase shift given by

$$\Delta\phi = -\phi_b - \phi_t + \sum_i \frac{4\pi n_i d_i \cos(\theta_{org,i})}{\lambda}, \quad (2)$$

where $\Delta\phi=2\Pi m$ with m=0, 1, 2…, d_i is the thicknesses of layers, and n_i is the refractive indices of organic layers. θ is the viewing angle, and $\theta_{org,i}$ is the propagation directions within the organic layers.

Luminance characteristics shown in Fig.4 can be defined as intensity of the emitted light per unit area in a given direction. Current efficiency is the amount of current flowing from the device with current density J. If the emissive area is S, with luminance L, I is the current then current efficiency n_L can be given by[18]

$$n_L = \frac{L}{J} = \frac{LS}{I}. \quad (3)$$

Luminous efficacy can be given by the ratio of optical flux to electrical input. If n_L is the current efficiency at applied voltage V_i, then it is denoted by n_p given by

$$n_p = \frac{n_L f_D \pi}{v_i}, \quad (4)$$

where f_D is the angular distribution of the emitted light in the forward hemisphere considering angles θ and ϕ then it can be given by

$$f_D = \frac{i}{\pi I_0} \iint I(\theta,\phi) \sin\theta \mathrm{d}\phi \mathrm{d}f_D, \quad (5)$$

where $I(\theta, \phi)$ is the intensity of light in the forward direction already given by Eq.(1).

Maximum luminance shown by device A is very low which is about 1 135 cd/m^2 at an applied voltage of 12 V. Device B which consists of Alq_3 doped with DCJTB in place of rubrene acts as ET-YEML has a yellow-green emission at about 500 nm and MS-TPD doped with BAlq as HT-BEML exhibits a blue emission at about 630 nm wavelength also emits white light with CIE coordinates of (0.318, 0.358). Device B shows a better luminance as compared with device A which is 3 825 cd/m^2 at the same applied voltage. Device C consists of Alq_3 doped with DCJTB acts as ET-YEML has a yellow-green emission at about 490 nm and CBP doped with BAlq as HT-BEML exhibits a blue emission at about 630 nm which is also a white OLED and has CIE coordinates at (0.31, 0.32). It has further enhancement in luminance which is about 5 430 cd/m^2. Device D has the best luminance performance of all the devices discussed. It also emits white light with ET-YEML as Alq_3 doped with DCJTB which is responsible for yellow-green emission at about 490 nm wavelength and HT-BEML as NPB doped with BAlq which emits blue light at 630 nm. It has CIE coordinates at (0.32, 0.31) and maximum luminance of 10 000 cd/m^2 at an applied voltage of 12 V. Fig.4 clearly indicates that device D has best luminance of all the devices discussed here. A summary of performance characteristics has been shown in Tab.1. Tab.1 indicates that device D has the maximum luminous efficacy of 15.25 lm/W which is comparable to that reference device (device without phase separation polymer) in Ref.[10].

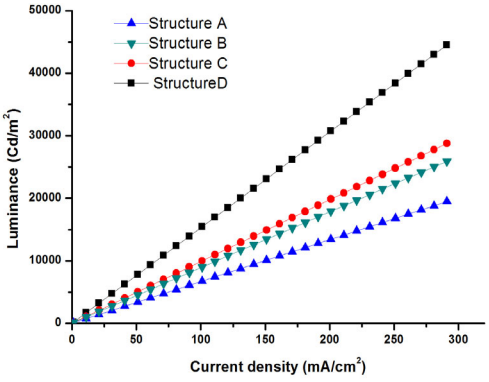

Fig.4 Luminance versus current density curve

From the description of all devices discussed above, device A has the lowest luminance among all other devices. This might be due the presence of rubrene doping in ET-YEML layer. This can be explained with the reasons, like (i) doping the device with rubrene will result in moving the emission zone towards the cathode which further results in fluorescence quenching[4], (ii) doping the device with rubrene will hinders the transport of electrons which decreases the carrier balance of the device[2], (iii) spectra of Rubrene doped devices changes with change in applied voltage due to the hole trapping nature of this material[11].

To further find out the effect of rubrene doping in Alq_3 in this device, simulation comparison with the following structure has been carried out:

Structure for Device E is Ca (20 nm)/ Alq_3 (60 nm)/ CBP: BAlq (50 nm)/ Al (60 nm)/ glass substrate.

Fig.5 shows that impedance of device B where Alq_3 is doped with rubrene has slightly high impedance as compared to device E impedance where Alq_3 is used as ETL.

This shows that transport of electrons in device B is inferior to electron transport of device E. This is because of negative effect of rubrene doping on the electron mobility of Alq_3. Hence it can be clearly concluded that rubrene doping deteriorates the device performance. Also, there is a decrease of impedance as the voltage increases. It indicates a transition in the device from insulating state to the conducting state[3].

Tab.1 The EL performance parameters summary of white OLED devices A—D

Device/ Characteristic	Maximum current density at 10 V (mA/cm^2)	Luminance (cd/m^2)	Luminous efficacy (lm/W)	CIE coordinates	Current efficiency (cd/A)
Device A	17	1 135	193	(0.32, 0.336)	6.69
Device B	43	3 825	269.5	(0.318, 0.358)	8.9
Device C	55	5 430	248.8	(0.317, 0.327)	9.89
Device D	64	10 000	237.3	(0.329, 0.312)	15.25

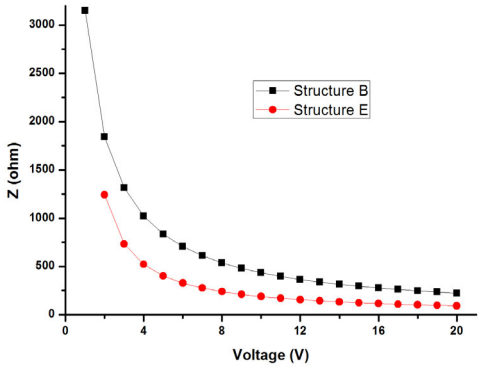

Fig.5 *Z-V* characteristic comparison for structure B and E

Fig.6 shows the I-V characteristics of structure B and E. While comparing, Fig.6 indicates that structure B requires high driving voltage as compared to structure E (structure without rubrene doping) to reach the same current. This indicates that doping of Rubrene in Alq_3 hinders the electron mobility of the Alq_3[3].

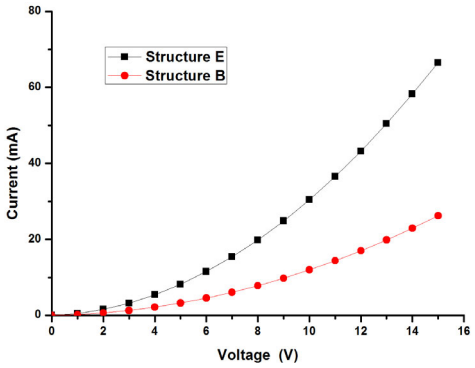

Fig.6 *I-V* characteristic comparison for structures B and E

Fig.7 shows the J-V curves of all the devices A-D. From the figure it can be concluded that the device which has NPB doped with DCJTB as HTL has the best current density characteristics with respect to the applied voltage. This can be attributed to the dramatic reduction in the hole injection barrier of the device after doping with DCJTB. The injection barrier could reduce from 0.1—0.2 eV, which can be clearly seen from Fig.2, while moving from device B to device D. Hence, DCJTB in NPB as a dopant is further improving the transport of holes by increasing the mobility and current density[12]. Enhancement in current density of device D with respect to other devices indicates improved hole injection and transport characteristics. Also, rubrene doping in ET-YEML in device A is responsible for an increase in operating voltage of the device due to interruption in electron transport[13].

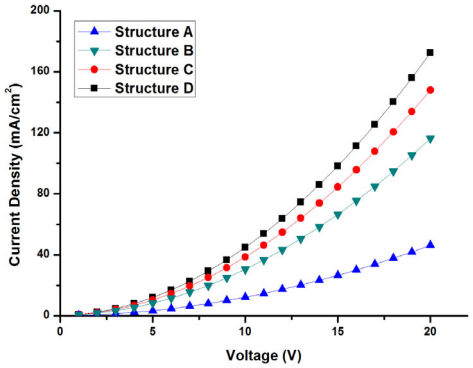

Fig.7 *J-V* characteristic comparison of devices A-D

We have also simulated for the dipole lifetime of the devices shown in Fig.1. This structure consists of two emission layers, i.e., ET-YEML and HT-BEML. The materials in the emission layer include Alq_3 doped with DCJTB or rubrene as ET-YEML and NPB, CBP or MS-TPD doped with BAlq as HT-BEML. Here we are calculating lifetime with a layer (HTL) thickness sweep from 1 nm to 100 nm. Resulting lifetime variations are shown in Fig.8 with respect to the HTL thickness variant.

Fig.8 indicates that device A, i.e., rubrene doped HTL has the longest excited state lifetime[14]. The oscillations of a dipole lifetime depend on the position of dipole with respect to the metal interface. These oscillations are more if it is near to the metal surface and vice-versa. Thus, nearby interfaces can cause changes in the lifetime which can be determined by reflected field at the emitter position. A scalar description of reflected field can be given

by[15,16]

$$\ddot{p}(t)+b\dot{p}(t)+w^2 p(t)=\frac{e^2}{m}E_{\mathrm{R}}(t), \tag{6}$$

where E_{R} denotes the reflected electric field, p is the scalar dielectric dipole moment, b is the decay rate which is also known as inverse lifetime, m is the mass of the oscillating dipole, e is the charge, and w is the angular frequency.

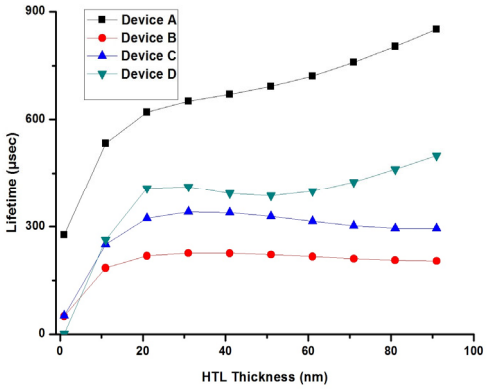

Fig.8 Lifetime versus HTL thickness variation

We have simulated a proposed top-emitting bi-layer phosphorescent white OLED with configuration Ca/ ET-YEML (yellow-green dopant)/ HT-BEML (blue dopant)/ Al/ Glass Substrate having four different structures as white OLEDs. NPB doped with BAlq shows the best device performance with luminance 10 000 cd/m^2 and current efficiency of 15.25 cd/A while rubrene doping in Alq_3 shows hindrance in the device performance. The devices simulated here can be used in application like solid state lighting because of high luminous efficacy at a low driving voltage. Device B is proved to be best for such applications since it has the highest luminous efficacy of all other devices, i.e., 269.5 lm/W. The luminous efficacy (lm/W) of device D is found comparable with that of Ref.[10].

Acknowledgement

Authors want to express their thanks to Amity University, Noida for supporting this work. Authors also like to express their gratitude to Fluxim for providing evaluation permission.

References

[1] P. Chen, R. Sheng, M. Ko, Y. Duan, G. Cheng and C. Che, Journal of Material Chemistry C **6**, 9890 (2018).
[2] K. L. Chen, Journal of Nanomaterials **2014**, 173276 (2014).
[3] B. Mo, X. Zhang, L. Liu, H. Wang, J. Xu, H. Wang and B. Wei, Optics & Laser Technology **68**, 202 (2015).
[4] H. Choukri, A. Fischer, S. Forget, S. Chénais, M. C. Castex, D. Adès, A. Siove and B. Geffroy, Applied Physics Letters **89**, 183513 (2006).
[5] J. Vollbrecht, New Journal of Chemistry **42**, 11249 (2018).
[6] S. Zou, Y. Shen, F. Xie, J. Chen, Y. Li and J. Tang, Materials Chemistry Frontiers **4**, 1089 (2020).
[7] B. C. Krummacher, V. E. Choong, M. K. Mathai, S. A. Choulis, F. So, F. Jermann, T. Fiedler and M. Zachau, Applied Physics Letters **88**, 113506 (2006).
[8] C. Murawski, C. Fuchs, S. Hofmann, K. Leo and M. C. Gather, Applied Physics Letters **105**, 113303 (2014).
[9] J. Lee, Woo J. Sung, C. W. Joo, H. Cho, N. Cho, G. W. Lee, D. H. Hwang and J. I. Lee, ETRI Journal **38**, 2 (2016).
[10] T.T.K. Tu, J. W. Han, D. J. Lee, D. W. kim, H. E. Park,Y. H. Kim and K. T. Lim, Optik **192**, 162944 (2019).
[11] W. Chen, L. Lu and J. Cheng, Optik **121**, 107 (2010).
[12] Z. Gao, Z. Feng, W. Chen, W. Qu, W. Ao, T. Yang, J. Li and F. Gao, RSC Advances **9**, 4957 (2019).
[13] B. C. Kwack, K. S. Lee, D. C. Choo, T. W. Kim, J. H. Seo and Y. K. Kim, Journal of Nano-science and Nanotechnology **8**, 5532 (2008).
[14] Y. Guang, S. L. Zhao, X. Zheng, F. J. Zhang, K. Chao, H. N. Zhu, D. D. Song and X. R. Xu, Chinese Physics B **19**, 037804 (2010).
[15] N. Danz, R. Waldhäusl, A. Bräuer and R. Kowarschik, Journal of Optical Society of America B **19**, 412 (2002).
[16] R. Ruppin and O. J. F. Martin, The Journal of Chemical Physics **121**, 11358 (2004).
[17] Michael Thomschke, Robert Nitsche, Mauro Furno and Karl Leo, Applied Physics Letters **94**, 083303 (2009).
[18] Daniel de Sá Pereira1, Przemyslaw Data and Andrew P. Monkman, Display and Imaging **2**, 323 (2017).
[19] S.-J. Yeh, M.-F. Wu, C.-T. Chen, Y.-H. Song, Y. Chi, M.-H. Ho, S.-F. Hsu and C. H. Chen, Advanced Materials **17**, 285 (2005).
[20] N. R. Park, G. Y. Ryu, D. H. Lim, S. J. Lee, Y. K. Kim, and D. M. Shin, J. Nanosci. Nanotechnol. **14**, 5109 (2014).